



Combination of off-line two-dimensional hydrophilic interaction liquid chromatography for polar fraction and two-dimensional hydrophilic interaction liquid chromatography \times reversed-phase liquid chromatography for medium-polar fraction in a traditional Chinese medicine

Zheng Liang, Kuiyong Li, Xinliang Wang, Yanxiong Ke, Yu Jin*, Xinmiao Liang*

Engineering Research Center of Pharmaceutical Process Chemistry, Ministry of Education, School of Pharmacy, East China University of Science and Technology, 130 Meilong Road, Shanghai 200237, China

ARTICLE INFO

Article history:

Received 9 October 2011
Received in revised form 3 December 2011
Accepted 13 December 2011
Available online 19 December 2011

Keywords:

Two-dimensional liquid chromatography
2-D HILIC \times HILIC
2-D HILIC \times RP-LC
Traditional Chinese medicine
Orthogonality
Peak capacity

ABSTRACT

Two-dimensional liquid chromatography (2-D LC) has been widely used for the analysis of complex samples owing to its great improvement in separation selectivity and peak capacity. However, one 2-D LC system may not be enough to meet the separation requirements due to the complexity of certain samples and respective limitations of two separation modes. In this work, water extract of *Scutellaria barbata* D. Don, a traditional Chinese medicine, was fractionated into polar fraction and medium-polar fraction by means of solid phase extraction (SPE). The fraction preparation made it easy to select the corresponding combination of 2-D LC method from hydrophilic interaction chromatography (HILIC) and reversed-phase liquid chromatography (RP-LC). An off-line 2-D HILIC \times HILIC to analyze the polar fraction and an off-line 2-D HILIC \times RP-LC to analyze the medium-polar fraction were developed, respectively. In total, 749 peaks were detected: 206 peaks from the polar fraction by the 2-D HILIC \times HILIC and 543 from the medium-polar fraction by the 2-D HILIC \times RP-LC. The practical peak capacities obtained in both systems were 2698 and 2879, and the orthogonality reached 63.18% and 90.62%, respectively. The results demonstrated that the two systems were both highly orthogonal, and the peak capacities greatly increased.

© 2012 Elsevier B.V. All rights reserved.

1. Introduction

Traditional Chinese medicine (TCM) commonly contains numerous components with diverse polarity, which often represents a great challenge for chromatographic analysis. Though high performance liquid chromatography (HPLC) is one of the most effective separation methods, its limitations in performance, selectivity and peak capacity are gradually found for the analysis of complex samples.

At present, comprehensive analysis of TCM increasingly relies on two-dimensional liquid chromatography (2-D LC) technique, an effective method to increase peak capacity and resolution. For a 2-D LC separation, the maximum theoretical peak capacity is the product of the peak capacities obtained on each of the two dimensions [1]. Besides, orthogonal separation based on different separation mechanisms could improve separation selectivity and facilitate the analysis of much more components in TCM. Different separation modes can be combined to construct a 2-D LC method according to the sample properties. Two-dimensional reversed-phase

liquid chromatography/reversed-phase liquid chromatography (2-D RP \times RP-LC) [2–7] has been the wide mode for TCM. For better orthogonality with traditional C18, some new stationary phases have been prepared and applied in 2-D RP \times RP-LC systems. A novel click oligo (ethylene glycol) (Click OEG) stationary phase was combined with C18 to develop a 2-D RP \times RP-LC system for analyzing *Lignum Dalbergiae Odoriferae* [2]. A highly orthogonal off-line 2-D RP \times RP-LC system developed from Click dipeptide stationary phase and C18, was used to analyze *Rheum Palmatum* L. [4]. Although 2-D RP \times RP-LC is very effective in the characterization of medium and weak polar components in TCM, it is invalid for polar components since these are poorly eluted under RP-LC mode. Thus the information of these polar components is frequently ignored when a 2-D RP \times RP-LC method is employed. Recently, hydrophilic interaction liquid chromatography (HILIC) has been steadily gaining interest and widely used for the analysis of polar compounds [8–10]. 2-D HILIC \times HILIC systems were also conducted to improve the separation for polar components in TCM. Xu et al. developed a comprehensive HILIC \times HILIC-MS system to separate and identify saponins from *Quillaja saponaria* [11]. Subsequently, Liu et al. developed two different off-line 2-D HILIC \times HILIC systems for the analysis of polar components in *Carthamus tinctorius* Linn. [12]. HILIC offers selectivity complementary to traditional RP-LC since

* Corresponding authors. Tel.: +86 021 64250633; fax: +86 021 64250622.
E-mail addresses: Jiny@ecust.edu.cn (Y. Jin), liangxm@ecust.edu.cn (X. Liang).

their good orthogonality [13–16]. Liu et al. developed an off-line RP-LC \times HILIC system based on C18 and Click β -cyclodextrin (β -CD) stationary phases, showing excellent abilities for the separation of medium-polar components in *C. tinctorius* Linn. [13]. Even though the 2-D RP-LC \times HILIC system could separate medium-polar and weak-polar components in the first dimension (RP-LC), medium-polar and polar components in the second dimension (HILIC) and could solve the problem of peak capacity and separation selectivity to some extent, there were still certain deficiencies by any single 2-D LC for comprehensive characterization of TCM samples due to limitations of separation modes and complexity of samples. The aim of this study was to divide a TCM extract into several fractions according to chromatographic polarity, followed by the development of an appropriate 2-D LC system for each fraction. The described combination of 2-D LC systems represents a more promising approach for the analysis of complex TCM samples.

Scutellaria barbata D. Don has been used in TCM for a long time for the treatment of tumors, hepatitis, cirrhosis, and other diseases. Flavonoids are main bioactive components in *S. barbata* [17]. In this work, water extract of *S. barbata* D. Don was divided into two fractions with solid phase extraction (SPE) according to corresponding chromatographic polarity. Subsequently, an off-line 2-D HILIC \times HILIC and an off-line 2-D HILIC \times RP-LC were developed to analyze the two fractions. Such double off-line 2-D LC systems enabled a comprehensive study of the components in *S. barbata* D. Don.

2. Experimental

2.1. Apparatus and chemicals

The HPLC system (Agilent 1200, Agilent Technologies, Waldbronn, Germany) consists of a G1312B binary pump, a G1367C autosampler, a G1379B degasser, a G1316B automatic thermostatic column compartment and a G1315C diode array detection (DAD) system.

The Mass Spectrometry (MS) determination was performed on a Waters ACQUITY UPLCTM system equipped with a binary solvent manager and autosampler. The UPLC was interfaced through an electrospray ionization (ESI) ion source to quadrupole time-of-flight (Q-TOF) PremierTM mass spectrometer operating in positive mode (Waters MS Technologies, Manchester, UK).

Acetonitrile (HPLC grade) from TEDIA (OH, USA) was used for HPLC analysis. Formic acid (HPLC grade) was purchased from ACROS Organics (NJ, USA). Ammonium formate was purchased from Sigma–Aldrich (St. Louis, MO, USA). Methanol used for sample preparation was obtained from YuWang Chemical Reagent Factory (Shandong, China). Milli-Q ultrapure water (Billerica, MA, USA) was used throughout for solution preparation unless stated. *S. barbata* D. Don was collected in Henan province.

2.2. Sample preparation

15 g sample was ground into powder and decocted in 100 mL of water for 120 min. The decoction was filtrated out and the residue was decocted in another 100 mL of water for 90 min. The decoctions were combined and concentrated, and then methanol was added until the concentration of methanol reached 75%. After standing for 24 h in refrigerator at 4 °C, the supernatant was filtered. The filtrate was evaporated and the residue was dissolved in 10 mL of water. After centrifugation, the supernatant was filtered through a 0.45 μ m hydrophilic membrane prior to the injection for HPLC analysis.

Oasis[®] HLB cartridge (Waters, Milford, MA, USA) was first activated with methanol and equilibrated with water. Sample solution

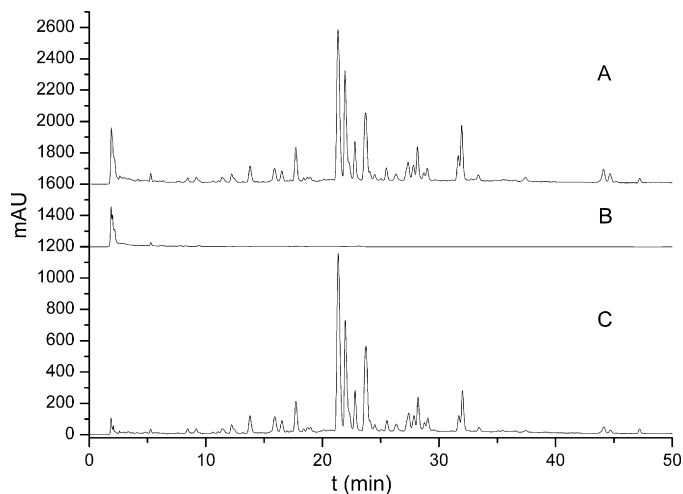


Fig. 1. The HPLC chromatograms of samples under RP-LC mode: (A) water extraction; (B) sample I (polar fraction); (C) sample II (medium-polar fraction). Column: XUnion C18 column (5 μ m, 150 mm \times 2.1 mm i.d.); Mobile phase: (A) water with 0.1% formic acid (B) acetonitrile with 0.1% formic acid; gradient: 0–40 min, 10–30% B, 40–50 min, 30–65% B; flow rate: 0.2 mL/min; temperature: 30 °C; UV detection: 280 nm.

(0.5 mL) was loaded onto cartridge and eluted with 10% methanol (5 mL) for polar fraction and 80% methanol (10 mL) for medium-polar fraction in sequence. This step was repeated four times and the respective fractions were combined. Then the combined fractions were evaporated to dryness and dissolved in 1 mL of water and 1 mL of CH₃OH/H₂O (50:50, v/v), and denoted as samples I and II, respectively. The samples were stored at 4 °C before use.

2.3. Chromatographic and MS conditions

In the 2-D HILIC \times HILIC analysis, an Atlantis HILIC Silica column (250 mm \times 4.6 mm i.d., 5 μ m particle size, Waters) was used as the first dimensional column. The corresponding mobile phase A was water with 5 mM ammonium formate (pH = 2.69), the mobile phase B was ACN/water (95:5, v/v) with 5 mM ammonium formate. The linear gradient was from 5% A to 40% A in 30 min at a flow rate of 1.0 mL/min. Fractions were collected manually from 3 to 20 min at 1 min intervals and they were denoted as fractions 1–18 in order. The fractions were evaporated to dryness under a nitrogen stream and the residue was dissolved in 200 μ L of ACN/water (50:50, v/v). The second dimensional analysis was performed on a XAmide column (150 mm \times 4.6 mm i.d., 5 μ m particle size, Sipore Co. Ltd.). The mobile phases and linear gradient used in the two dimensions were same. The injection volume was 20 μ L for the first dimension and 10 μ L for the second dimension, respectively.

In the 2-D HILIC \times RP-LC analysis, a XAmide column was taken as the first dimensional column. The corresponding mobile phase A was water with 0.1% (v/v) formic acid, and the mobile phase B was ACN with 0.1% (v/v) formic acid. The linear gradient was from 5% A to 40% A in 30 min at a flow rate of 1.0 mL/min. Fractions were collected manually from 2 to 21 min at 1 min intervals and they were denoted as fractions 1–20 in order. The fractions were evaporated to dryness under a nitrogen stream and the residue was dissolved in 200 μ L of CH₃OH/water (50:50, v/v). The second dimensional analysis was performed on a XUnion C18 column (150 mm \times 2.1 mm i.d., 5 μ m particle size, Sipore Co. Ltd.). The mobile phases used in the two dimensions were same. The linear gradient was from 10% B to 30% B in 40 min, and then reached 65% B at 50 min. The flow rate was 0.2 mL/min. The injection volume was 10 μ L for the first dimension and 5 μ L for the second dimension, respectively.

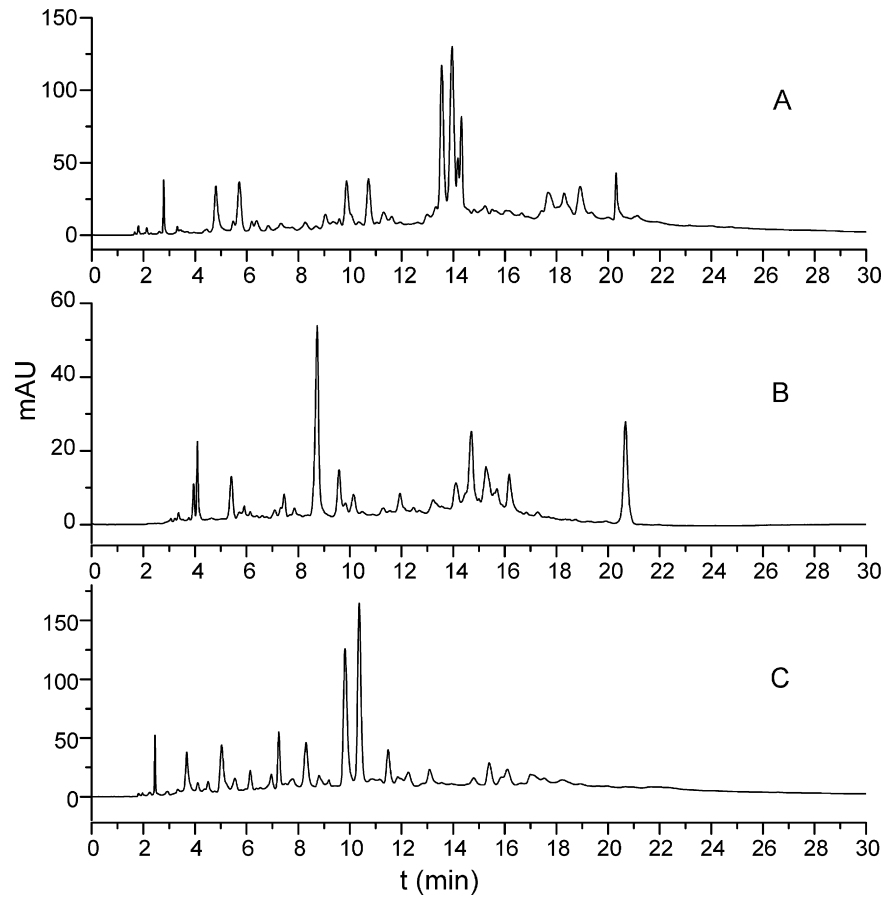


Fig. 2. The HPLC chromatograms of sample I under HILIC mode on (A) Click Maltose column ($5\ \mu\text{m}$, $150\ \text{mm} \times 4.6\ \text{mm}$ i.d.); (B) Atlantis HILIC Silica column ($5\ \mu\text{m}$, $250\ \text{mm} \times 4.6\ \text{mm}$ i.d.); (C) XAmide column ($5\ \mu\text{m}$, $150\ \text{mm} \times 4.6\ \text{mm}$ i.d.). Mobile phase: (A) water with 5 mM ammonium formate, pH = 2.69 (B) ACN/water (95:5, v/v) with 5 mM ammonium formate; gradient: 0–30 min, 5–40% A; flow rate: 1 mL/min; temperature: $30\ ^\circ\text{C}$; UV detection: 280 nm.

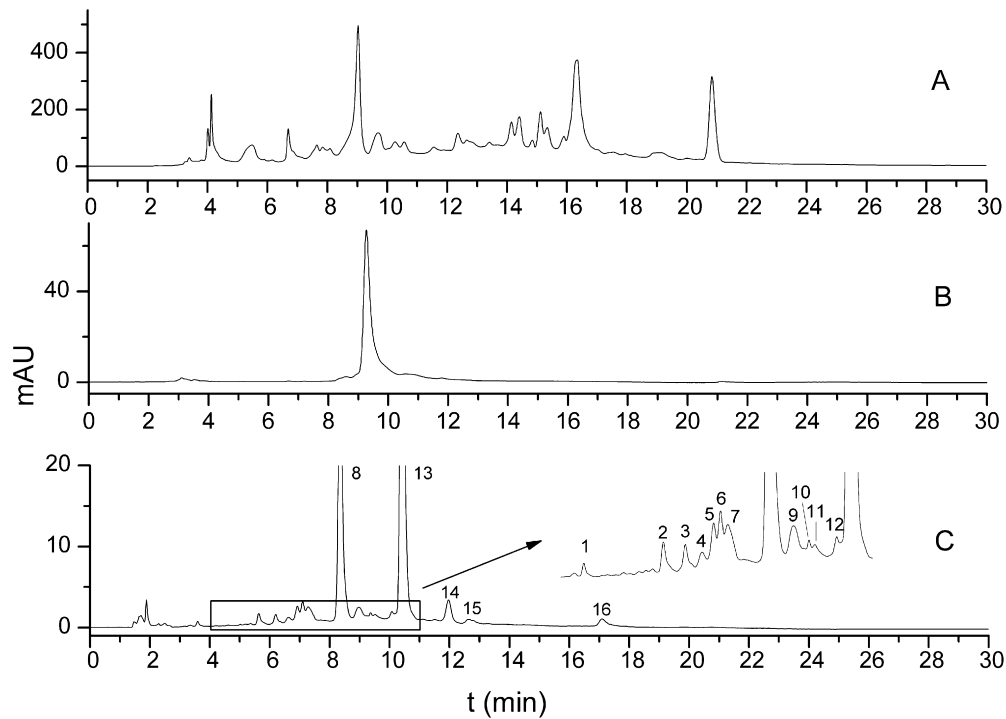


Fig. 3. Off-line 2-D HILIC \times HILIC analysis of preparative fraction 7. Chromatogram (A) was sample I on Atlantis HILIC Silica column; chromatograms (B) and (C) were fraction 7 (eluted between 9 and 10 min in the first dimension) on Atlantis HILIC Silica column and XAmide column, respectively. Detailed experimental conditions are given in Section 2.3.

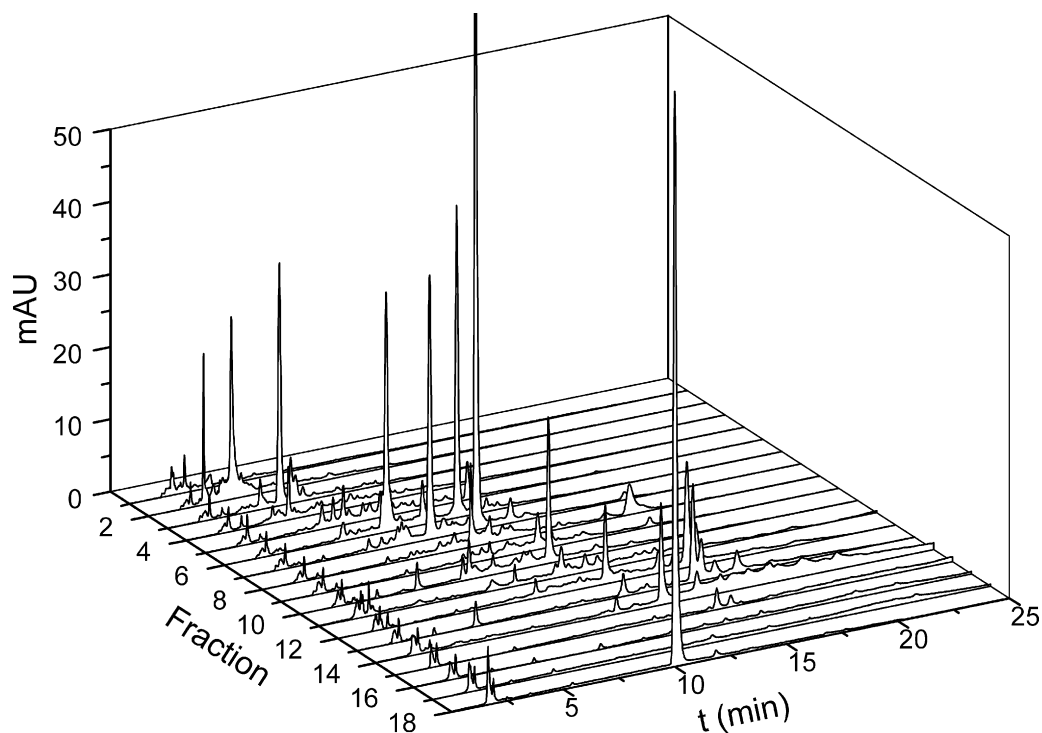


Fig. 4. Three-dimensional chromatogram of fractions 1–18 for sample I analyzed under HILIC mode on XAmide column.

In both of the two systems, the column temperature was 30 °C and the UV detection was set at 280 nm.

ESI-MS was performed on an ACQUITY UPLC BEH C18 (100 mm × 2.1 mm i.d., 1.7 μm particle size, Waters). The corresponding mobile phase A was water with 0.1% (v/v) formic acid, and the mobile phase B was ACN with 0.1% (v/v) formic acid. The linear gradient was from 10% B to 40% B in 20 min at a flow rate of 0.2 mL/min. ESI-MS and MS² parameters were as follows. The nebulization gas was set to 800 L/h, and the cone gas was set to 50 L/h. Source temperature and desolvation temperature were 120 °C and 380 °C, respectively. The capillary voltage was set to 3.0 kV, and the cone voltage was set to 25 V. The Q-TOF Premier acquisition rate was set to 1.0 s with a 0.02 s interscan delay. The scan range was 220–1000 *m/z*. Argon was employed as collision gas. All the analysis were acquired by using the lock spray to ensure accuracy and reproducibility; leucine-enkephalin was used as the lock mass at a concentration of 50 pg/μL and a flow rate of 10 μL/min, generating an [M+H]⁺ ion at 556.2771 Da. Data were collected in centroid mode and processed using MassLynx 4.1 software (Waters).

2.4. Data analysis

Orthogonality was evaluated according to a reported method [13,18]. This method is suitable for evaluating the orthogonality of unknown compounds. Retention time data in the second dimension are normalized according to Eq. (1),

$$t_R^{i(norm)} = \frac{t_R^i - t_R^{min}}{t_R^{max} - t_R^{min}} \quad (1)$$

where t_R^{max} and t_R^{min} represent the retention times for the peaks showing the greatest and the least retention among all the second dimension runs, respectively. The retention times t_R^i are converted to normalized $t_R^{i(norm)}$ values that range from 0 to 1. For the x-axis, the grid number is equal to the number of fractions in the first

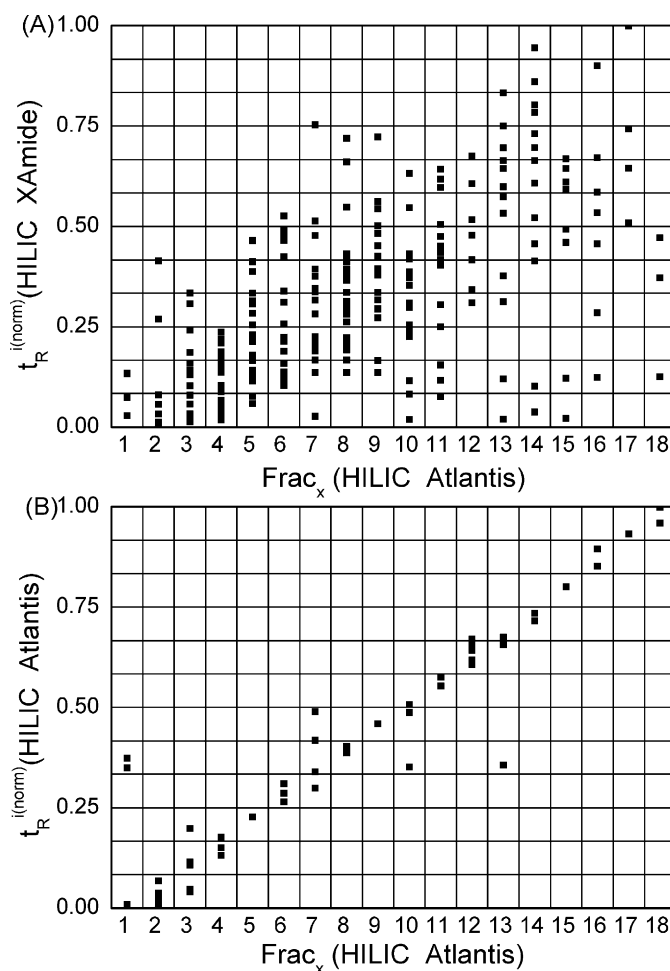


Fig. 5. Normalized plots for 2-D HILIC × HILIC system: (A) orthogonal HILIC × HILIC system; (B) non-orthogonal HILIC × HILIC system.

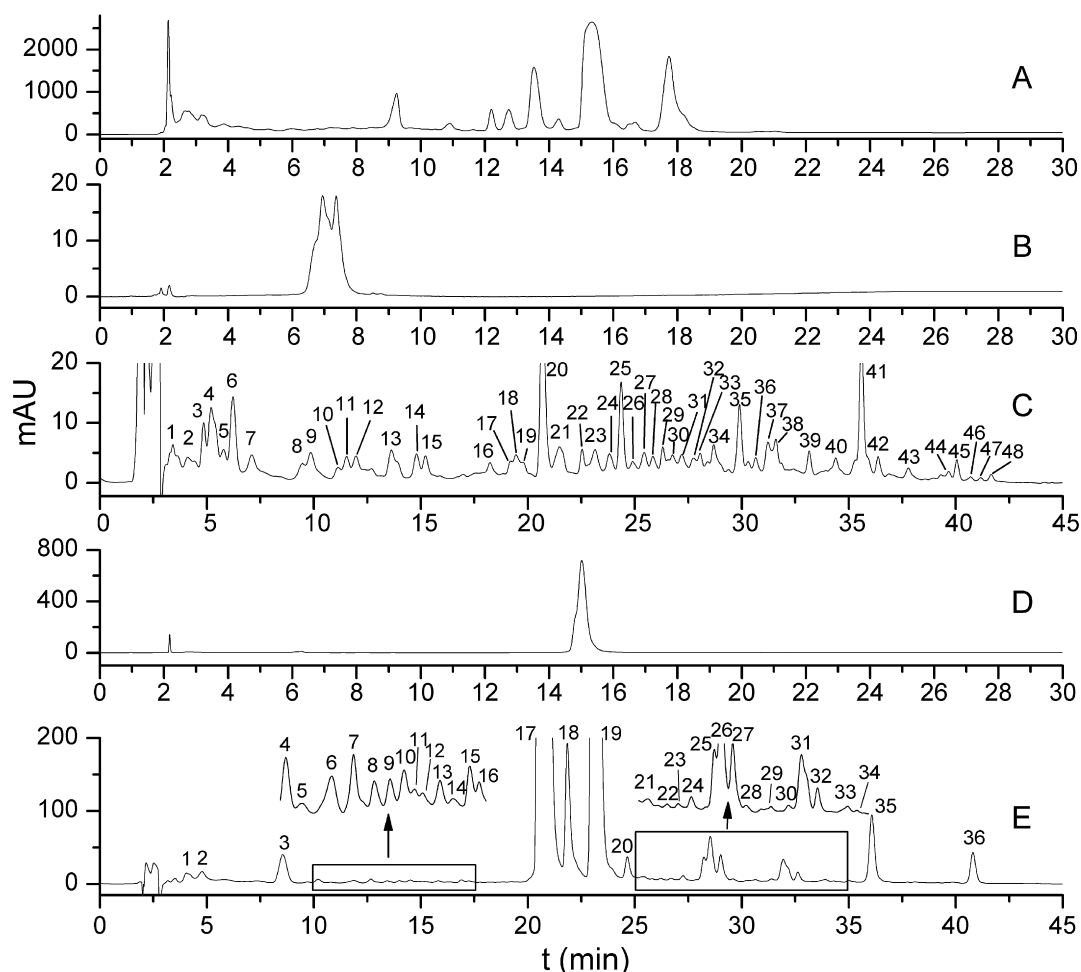


Fig. 6. Off-line 2-D HILIC \times RP-LC analysis of preparative fractions 6 and 14. Chromatogram (A) was sample II on XAmide column; chromatograms (B) and (C) were fraction 6 (eluted between 7 and 8 min in the first dimension) on XAmide column and C18 column, respectively; chromatograms (D) and (E) were fraction 14 (eluted between 15 and 16 min in the first dimension) on XAmide column and C18 column, respectively. Detailed experimental conditions are given in Section 2.3.

dimension. For the y -axis, the grid number is defined according to Eq. (2),

$$\text{Grid}_y = \frac{\text{Num}_p}{\text{Frac}_x} \quad (2)$$

where Num_p is the number of peaks detected by the 2-D LC method and Frac_x is the grid number of the x -axis. The more complex of a sample is, the more bins should be given, thus the degree of coverage can describe the orthogonality. The orthogonality was calculated according to Eq. (3),

$$\text{O\%} = \frac{\sum \text{bins} - \sum \text{bins}(\text{blank})}{0.63P_{\max}} \times 100 \quad (3)$$

where $\sum \text{bins}$ is the number of bins in the 2D plot containing data points and P_{\max} is the total peak capacity obtained as the sum of all bins. $\sum \text{bins}(\text{blank})$ is the number of bins containing data points in the 2D plot when the fractions are re-injected on the first dimensional column, i.e., a non-orthogonal system, in which the data points would be lined up along the diagonal, and the surface coverage should be 10%.

The total peak capacity of 2-D LC is the product of the peak capacities of the first and second dimensions under ideal conditions. Practical peak capacity (N_p) of system for complex sample can be calculated according to Eq. (4) by the knowledge of surface

coverage [18], where P_1 and P_2 are peak capacities of both separation dimensions:

$$N_p = P_1 P_2 \frac{\sum \text{bins}}{P_{\max}} \quad (4)$$

However, the practical peak capacity is also influenced by the sampling rate of first dimension peaks, where under-sampling occurs. According to the theoretical work in previous study [19,20], the effective 2D peak capacity (defined as $n'_{c,2-D}$) can be calculated according to Eq. (5) taking under-sampling effect into account:

$$n'_{c,2-D} = \frac{{}^1n_c {}^2n_c}{\sqrt{1 + 3.35({}^2t_c {}^1n_c / {}^1t_g)^2}} \quad (5)$$

Here 1n_c and 2n_c are peak capacities in first and second dimensions, respectively, 2t_c and the second dimension cycle time and 1t_g the first dimension gradient time. The fraction collection time, 1 min, is substituted for the second dimension cycle time (2t_c) since in our case off-line 2-D analyses were performed.

3. Results and discussion

3.1. Design of double off-line 2-D LC systems

Water extract of *S. barbata* D. Don was first analyzed under RP-LC mode (Fig. 1A) with polar components eluted at the dead

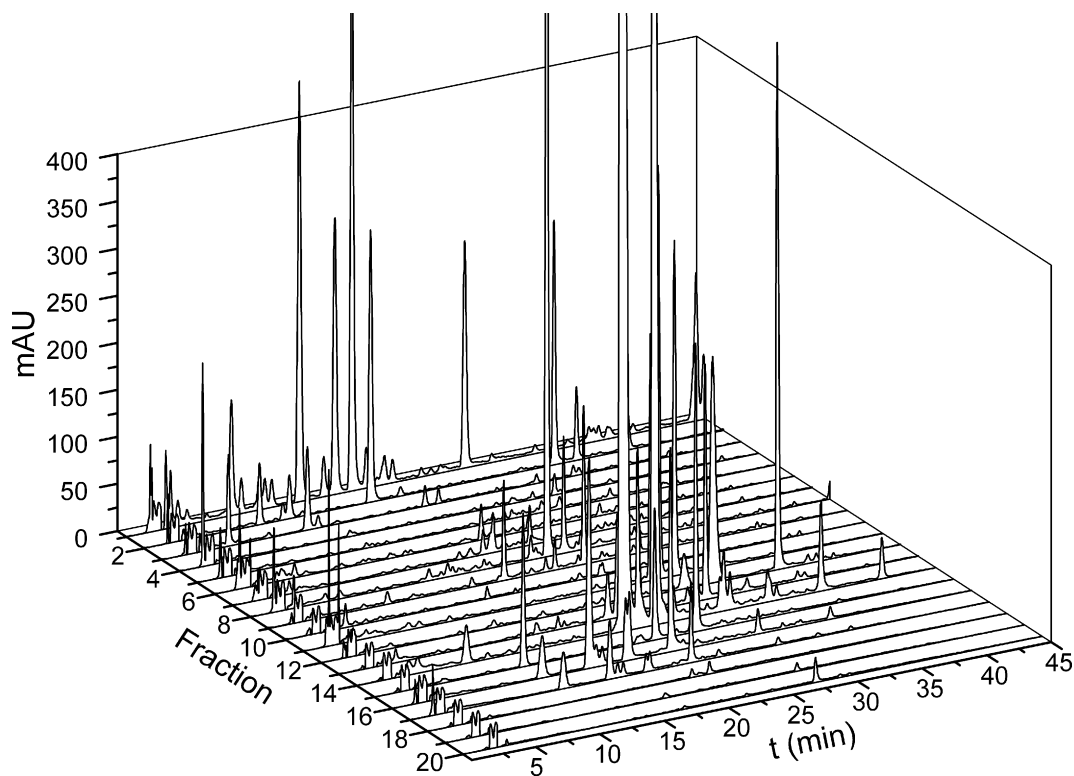


Fig. 7. Three-dimensional chromatogram of fractions 1–20 for sample II analyzed on C18 column.

time. After SPE pretreatment, the sample was divided into two fractions according to chromatographic polarity: the polar fraction eluted with 10% methanol (sample I, Fig. 1B) and the medium-polar fraction eluted with 80% methanol (sample II, Fig. 1C). As can be seen in Fig. 1B, the polar fraction was a co-eluted peak at the dead time under RP-LC mode. Obviously sole RP-LC was unable to analyze the obtained water extract. Polar compounds have good retention under HILIC mode. So polar fraction was obtained by SPE pretreatment, and then a 2-D HILIC \times HILIC system was designed for the analysis of polar fraction. Moreover, most of medium-polar components in *S. barbata* are flavonoid glycosides, which have good retention under both RP-LC and HILIC modes. Therefore, a 2-D HILIC \times RP-LC system was designed to analyze medium-polar fraction. Moreover, the off-line mode has no restrictions on the second dimension analysis time, so the fractions eluted from the first dimension could be prepared and analyzed with enough time. From this point of view, fractions can be well separated in the second dimension which is beneficial to the assessment of 2-D LC systems constructed here. Therefore, to maximally increase the resolving power of two dimensions, off-line mode was chosen. By combining the two off-line 2-D LC systems, components in *S. barbata* were further investigated.

3.2. Off-line 2-D HILIC \times HILIC analysis for sample I

3.2.1. Separation results for 2-D HILIC \times HILIC system

Three kinds of columns with different polar stationary phases, Click Maltose column, Atlantis HILIC Silica column and XAmide column were selected here. Mobile phases were optimized as follows. 0.1% Formic acid was initially used to the mobile phase, and the retention of the analytes was weak and the peak shape was observed to be poor. 10 mM ammonium formate in water phase was then tried. Although the retention and peak shape were slightly improved to some extent, the baseline was not stable due to the

change of buffer concentration in the gradient time. Finally, 5 mM ammonium formate was added in both phases and pH was adjusted to 2.69 as described in Section 2.3 to make the concentration of buffer constant in the whole analysis time. Three kinds of columns were investigated under the last optimal condition. In general, a single peak eluted at the dead time under RP-LC mode revealed vast peaks under HILIC mode. It also can be seen from Fig. 2 that the sample exhibited good retention on all three columns, and the peak shape and efficiency on XAmide column were better than the others. In terms of the separation selectivity, Click Maltose column and XAmide column were similar, which could be visually seen from Fig. 2A and C. By comparing Fig. 2B with Fig. 2C, the chromatogram patterns of sample I on silica column and XAmide column were entirely different indicating their good orthogonality. In view of its higher separation efficiency, better resolution and peak shape, the XAmide column was chosen as the second dimensional column for further separation, while Atlantis HILIC Silica column as the first dimensional column in the 2-D HILIC \times HILIC system.

In our experiments, the analysis of the 18 fractions eluted from the Atlantis HILIC Silica column was performed under the same gradient condition as that on the XAmide column, and the chromatograms showed many peaks, indicating high orthogonality of this 2-D HILIC \times HILIC system. Taking fraction 7 as an example, when the fraction was re-injected onto the Atlantis HILIC Silica column, only one peak was apparent (Fig. 3B). However, orthogonal analysis in the second dimension showed that 15 peaks dispersed throughout the chromatogram (Fig. 3C), which indicated that low abundance peaks co-eluted with the major peak in the first dimensional separation could be well resolved by the orthogonal separation. The highly orthogonal 2-D LC systems could detect the low-abundance components in the complex sample more efficiently. So this orthogonal 2-D LC system can facilitate the separation of more components from a sample. A three-dimensional chromatogram was constructed to illustrate the 2-D HILIC \times HILIC

analysis of sample I (Fig. 4). The polar fraction seemed to be very simple under RP-LC mode, but many components were revealed with good retention and separation on both dimensions by employing such a 2-D HILIC \times HILIC system.

3.2.2. Orthogonality and practical peak capacity of the 2-D HILIC \times HILIC system

Using the evaluation method described in Section 2.4, the orthogonality of the 2-D HILIC \times HILIC for the separation of sample I was investigated. In this work, 206 peaks were detected in the 18 fractions. As shown in Fig. 5A, the plot was divided into 18×12 bins (216, which approximates to 206), and bins containing data points were 111. While calculating $\sum \text{bins}(\text{blank})$, the non-orthogonal system was developed by the re-analysis of the 18 fractions in the first dimension, and the plot was constructed with the same division. As shown in Fig. 5B, $\sum \text{bins}(\text{blank})$ was 29. According to Eq. (3) the value of $O\%$ was 63.18% in this separation.

The baseline peak width on the Atlantis HILIC Silica column was approximately 0.24 min at a flow rate of 1 mL/min, representing a peak capacity of 125 in a 30-min analysis. The average baseline peak width on the XAmide column was approximately 0.18 min, representing a peak capacity of 166. Therefore, the practical peak capacity of 2-D HILIC \times HILIC was 11,181 when calculated according to Eq. (4). However, it was over-estimated due to failure to take under-sampling into account; for example, some separated peaks in the first dimension were re-combined in the collected fractions before injection into the second dimension. When considering this phenomenon, the practical peak capacity was 2698 according to Eq. (5). Obviously, the big difference of these two results demonstrated under-sampling cannot be ignored in assessing the peak capacity of 2-D LC. Even though the calculated practical peak capacity decreased to 2698, it still represented a great improvement of separation power in such a 2-D HILIC \times HILIC system.

3.3. Off-line 2-D HILIC \times RP-LC analysis for sample II

3.3.1. Separation results for 2-D HILIC \times RP-LC system

In the first dimension, XAmide column was selected to separate sample II under HILIC mode. As shown in Fig. 6A, the sample exhibited good retention on the XAmide column. Due to the different retention mechanisms between HILIC and RP-LC, a traditional C18 column was employed on the second dimension with effective separation results. Less than two peaks were separated by re-analysis of fraction 6 on the XAmide column (Fig. 6B). However, orthogonal analysis in the second dimension showed that 48 peaks buried in the baseline in the first dimensional analysis dispersed throughout the chromatogram (Fig. 6C). When fraction 14 was re-injected onto the XAmide column, only one peak was apparent (Fig. 6D); however, the analysis in the second dimension revealed a chromatogram containing 36 peaks (Fig. 6E). A three-dimensional chromatogram was also constructed to illustrate the 2-D HILIC \times RP-LC analysis of sample II (Fig. 7), which showed high resolving power of this system.

3.3.2. Orthogonality and practical peak capacity of the 2-D HILIC \times RP-LC system

In this work, 543 peaks were detected in 20 fractions totally. As shown in Fig. 8A, the plot was divided into 20×28 bins (560, which approximates to 543), and bins containing data points were 347. $\sum \text{bins}(\text{blank})$ calculated with the method was described in Section 3.2.2. As shown in Fig. 8B, $\sum \text{bins}(\text{blank})$ was 37. According to Eq. (3) the value of $O\%$ reaches 90.62%, which revealed high orthogonality in this separation.

The peak width at baseline on the XAmide column was approximately 0.30 min at a flow rate of 1 mL/min, which represented a peak capacity of 100 in 30 min. The average baseline peak width on

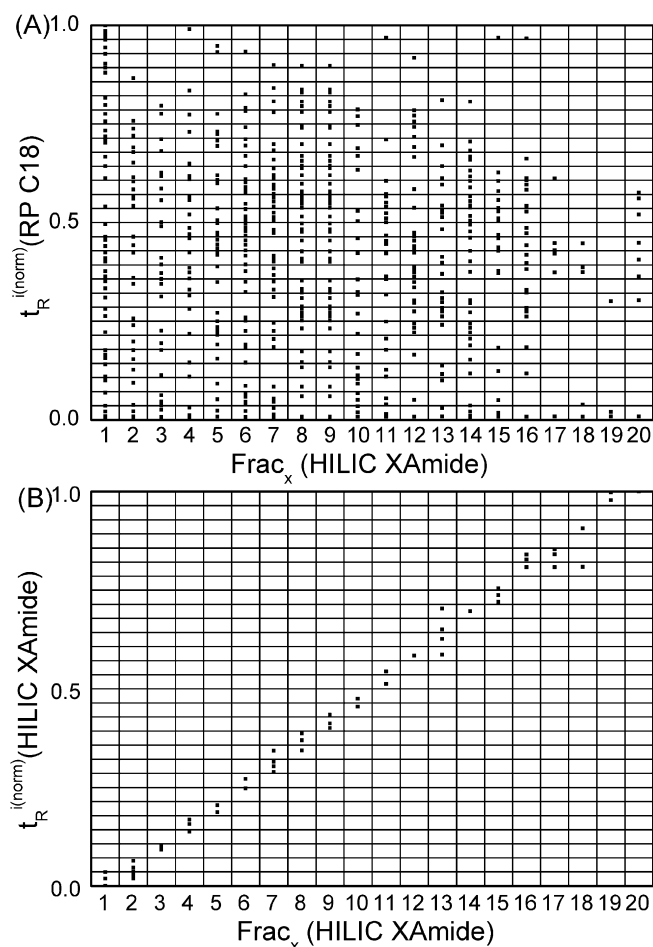


Fig. 8. Normalized plots for 2-D HILIC \times RP-LC system: (A) orthogonal HILIC \times RP-LC system; (B) non-orthogonal HILIC \times HILIC system.

the C18 column was approximately 0.28 min, representing a peak capacity of 178 in 50 min. As the discussion in 3.2.2, the practical peak capacity of this system was 2879 calculated according to Eq. (5) while 11,375 according to Eq. (4). It was obvious that the resolution and peak capacity were greatly improved.

3.4. Characterization of flavonoids in medium-polar fraction

20 fractions of sample II were analyzed by ESI-MS. Generally, flavonoids have been regarded as the active ingredients of *S. barbata* and have always been paid more attention. In total, 22 flavonoids including 7 flavones and 15 flavonoid glucosides were tentatively identified by structural proposal with MS fragmentation rules (Table 1). However, identification of flavonoids only by MS is a challenge since the positions of hydroxyl groups are difficult to determine. Although the selected ion monitor (SIM) and collision-induced dissociation (CID) of some interested ions can be performed by MS, effective separation is still necessary to acquire more and better MS information. As shown in Table 1, retention times of compounds 9, 21 and 22 with the same m/z at 463 were 8.23 min, 8.34 min, and 8.19 min, but they were fractionated into fractions 7, 15 and 16 after the first dimensional separation, respectively. Thus, these three structural isomers whose retention times were very close in one-dimensional LC could be eluted into different fractions, and they can be detected obviously in the second dimensional separation. Therefore, structural isomers which have very close retention times were identified by such off-line 2-D LC system.

Table 1
Tentative identities of flavonoids detected in medium-polar fraction from *Scutellaria barbata* D. Don.

No.	Fraction	t_R (min)	UV (nm)	$[M+H]^+$ (m/z)	MS ² fragment ions	Possible structure
1	1	16.29	270, 326	301	MS ² [301]: 301(5), 286(100), 183(25), 168(29)	4'-Hydroxy-wogonin
2	1	16.31	292, 346 (sh)	273	MS ² [273]: 273(6), 153(100), 147(34), 119(26)	Naringenin
3	1	16.35	292, 349 (sh)	303	MS ² [303]: 303(8), 183(100), 168(34), 147(12)	5,7,4'-Trihydroxy-8-methoxyflavanone
4	1	16.39	262, 336	271	MS ² [271]: 271(20), 153(100), 145(14), 121(20), 119(40)	Apigenin
5	1	16.61	272, 326	301	MS ² [301]: 301(13), 286(100), 168(13)	5,7,2'-Trihydroxy-8-methoxyflavanone
6	2	11.57	290, 333	287	MS ² [287]: 287(12), 269(6), 213(6), 195(11), 169(27), 145(8), 123(100), 121(18), 119(39)	Scutellarein
7	2	13.71	260, 345	287	MS ² [287]: 287(23), 241(10), 213(7), 161(20), 153(100), 137(14), 135(31)	Luteolin
8	6	7.80	283, 345 (sh)	435	MS ² [435]: 273(100)	Naringin
9	7	8.23	263, 334	463	MS ² [273]: 153(100), 147(30), 119(20)	4'-Hydroxy-wogonin-7-O-glucoside
10	8	8.32	263, 337	433	MS ² [463]: 301(100) MS ² [301]: 286(100) MS ² [433]: 271(100)	Apigenin-7-O-glucoside
11	8	8.75	275, 335	449	MS ² [271]: 271(21), 243(5), 163(5), 153(100), 145(25), 121(20), 119(44) MS ² [449]: 287(100)	5,7,8,2'-Tetrahydroxyflavone-7-O-glucoside
12	9	6.83	264, 348	449	MS ² [287]: 287(16), 195(10), 169(27), 145(7), 123(100), 121(14), 119(34) MS ² [449]: 287(100)	Luteolin-7-O-glucoside
13	11	10.22	286, 349 (sh)	479	MS ² [287]: 287(20), 241(12), 213(6), 161(18), 153(100), 137(12), 135(30), MS ² [479]: 303(100) MS ² [303]: 303(5), 183(100), 168(30), 147(11)	5,7,4'-Trihydroxy-8-methoxyflavanone-7-O-glucuronide/5,7,4'-trihydroxy-8-methoxyflavanone-4'-O-glucuronide
14	11	10.52	284, 334 (sh)	449	MS ² [449]: 273(100) MS ² [273]: 153(100), 147(24), 119(15)	Naringenin-7-O-glucuronide
15	11	10.91	285, 349 (sh)	479	MS ² [479]: 303(100) MS ² [303]: 303(6), 183(100), 168(31), 147(12)	5,7,4'-Trihydroxy-8-methoxyflavanone-7-O-glucuronide/5,7,4'-trihydroxy-8-methoxyflavanone-4'-O-glucuronide
16	12	10.15	268, 334	447	MS ² [447]: 447(13), 271(100) MS ² [271]: 271(29), 243(5), 163(5), 153(100), 145(23), 121(22), 119(45)	Apigenin-7-O-glucuronide
17	12	10.39	273, 321	477	MS ² [477]: 477(9), 301(100) MS ² [301]: 301(5), 286(100)	4'-Hydroxy-wogonin-7-O-glucuronide
18	12	11.85	273, 334	463	MS ² [463]: 463(98), 287(100) MS ² [287]: 287(43), 259(8), 241(7), 213(10), 195(10), 169(100), 145(24), 123(75), 121(32), 119(77)	Scutellarin
19	14	8.21	287, 370 (sh)	465	MS ² [465]: 289(100) MS ² [289]: 169(100), 147(21)	Carthamidin-7-O-glucuronide/isocarthamidin-7-O-glucuronide
20	14	8.99	290, 370 (sh)	465	MS ² [465]: 289(100) MS ² [289]: 169(100), 147(22)	Carthamidin-7-O-glucuronide/isocarthamidin-7-O-glucuronide
21	15	8.34	260, 348 (sh)	463	MS ² [463]: 463(18), 287(100) MS ² [287]: 287(22), 241(9), 161(19), 153(100), 137(16), 135(44)	Luteolin-7-O-glucuronide
22	16	8.19	284, 338 (sh)	463	MS ² [463]: 463(11), 287(100) MS ² [287]: 287(16), 213(5), 195(8), 169(30), 145(7), 123(100), 121(13), 119(38)	5,8,2'-Trihydroxyflavone-7-O-glucuronide

Generally, numerous low-abundance compounds were found by our method to be non-flavonoids. Unfortunately, these compounds were difficult to be identified according to the current information achieved and more work is still needed.

4. Conclusions

In this work, two off-line 2-D LC systems were designed rationally to analyze a complex TCM sample-*S. barbata* D. Don. Water extract was first separated into two fractions by SPE according to chromatographic polarity. 206 peaks were detected in polar fraction by a 2-D HILIC \times HILIC of which the orthogonality reached 63.18%; 543 peaks were detected in medium-polar fraction by a 2-D HILIC \times RP-LC of which the orthogonality reached 90.62%. By combining such double 2-D LC systems, 749 peaks were separated and analyzed in *S. barbata* D. Don totally. Moreover, the calculated practical peak capacities in both systems were 2698 and 2879, respectively. The results demonstrated that these two systems were both highly orthogonal, and the peak capacities were greatly increased. The double off-line 2D-LC systems may have a great potential for the separation of complex samples of different polarities and contents.

Acknowledgments

This work was supported by the Ministry of Science and Technology of China (2009BADB9B02), National Natural Science Funds

for Distinguished Young Scholars (20825518) and National Natural Science Funds (21005028).

References

- [1] J.C. Giddings, J. High Resolut. Chromatogr. 10 (1987) 319.
- [2] Y. Liu, Z. Guo, Y. Jin, X. Xue, Q. Xu, F. Zhang, X. Liang, J. Chromatogr. A 1206 (2008) 153.
- [3] Y. Liu, Q. Xu, X. Xue, F. Zhang, X. Liang, J. Sep. Sci. 31 (2008) 935.
- [4] M. Xue, H. Huang, Y. Ke, C. Chu, Y. jin, X. Liang, J. Chromatogr. A 1216 (2009) 8623.
- [5] J. Zhang, Y. Jin, Y. Liu, Y. Xiao, J. Feng, X. Xue, X. Zhang, X. Liang, J. Sep. Sci. 32 (2009) 2084.
- [6] J. Zeng, Z. Guo, Y. Xiao, C. Wang, X. Zhang, X. Liang, J. Sep. Sci. 33 (2010) 3341.
- [7] G. Jin, Y. Dai, J. Feng, X. Qin, X. Xue, F. Zhang, X. Liang, J. Sep. Sci. 33 (2010) 564.
- [8] A.J. Alpert, J. Chromatogr. 499 (1990) 177.
- [9] T. Ikegami, K. Tomomatsu, H. Takubo, K. Horie, N. Tanaka, J. Chromatogr. A 1184 (2008) 474.
- [10] P. Jandera, Anal. Chim. Acta 692 (2011) 1.
- [11] Y. Wang, X. Lu, G. Xu, J. Chromatogr. A 1181 (2008) 51.
- [12] Y. Liu, Z. Guo, J. Feng, X. Xue, F. Zhang, Q. Xu, X. Liang, J. Sep. Sci. 32 (2009) 2871.
- [13] Y. Liu, X. Xue, Z. Guo, Q. Xu, F. Zhang, X. Liang, J. Chromatogr. A 1208 (2008) 133.
- [14] Y. Wang, X. Lu, G. Xu, J. Sep. Sci. 31 (2008) 1564.
- [15] Z. Guo, Y. Jin, T. Liang, Y. Liu, Q. Xu, X. Liang, A. Lei, J. Chromatogr. A 1216 (2009) 257.
- [16] K.M. Kalili, A. de Villiers, J. Chromatogr. A 1216 (2009) 6274.
- [17] X. Hu, J. You, C. Bao, H. Zhang, X. Meng, T. Xiao, K. Zhang, Y. Wang, H. Wang, H. Zhang, A. Yu, Anal. Chim. Acta 610 (2008) 217.
- [18] M. Gilar, P. Olivova, A.E. Daly, Anal. Chem. 77 (2005) 6426.
- [19] J.M. Davis, Anal. Chem. 80 (2008) 461.
- [20] X. Li, D.R. Stoll, P.W. Carr, Anal. Chem. 81 (2009) 845.